CHEMISTRY & BIOLOGY INTERFACE

An official Journal of ISCB, Journal homepage; www.cbijournal.com

Synthesis of novel Steroidal-naproxen prodrugs, their molecular docking and theoretical studies by quantum chemical calculation

Arun Sethi*[1], AkritiBhatia[1], Ranvijay Pratap Singh[1], Shipra Gupta[2]

[1]*Department of Chemistry, University of Lucknow, Lucknow 226007, U.P., India.*
[2]*Department of Bioinformatics, Pune University, Pune– 411007, Maharashtra, India.*
**Corresponding author:* E-mail: alkaarunsethi@rediffmail.com; Tel: 91-9415396239*

Abstract: Two new steroidal-NSAID prodrugs 3β–2–(6–methoxynapthalen–2–yl)–propioxy–5β–spirost–5–en(**1**)and20–oxo–pregn–5,16–diene–3β–yl–2–(6–methoxynapthalen–2–yl) propionate (**4**) have been synthesized by adopting Steglich esterification. The structures of all the compounds have been characterized with the help of ^{1}H and ^{13}C NMR, FT-IR, UV and mass spectrometry. Quantum chemical calculations have been performed by density functional theory (DFT) using B3LYP functional and 6-31G (d, p) basis set. ^{1}H and ^{13}C NMR chemical shift values have been evaluated using gauge-independent atomic orbital (GIAO). Stability of the molecules as a result of hyperconjugative interactions and electron delocalization were analyzed using natural bond orbital (NBO) analysis. The calculated HOMO-LUMO energies by TD-DFT showed that charge transfer takes place within the molecule.The strength and nature of weak intramolecular interactions have been studied by AIM approach. Global reactivity descriptors have been computed to predict reactivity and reactive sites in the molecule.The vibrational wavenumbers have been calculated using DFT method and assigned with the help of potential energy distribution (PED). First hyperpolarizability values have been calculated to describe the nonlinear optical (NLO) property of the synthesized compounds.Molecular electrostatic potential (MEP) analysis has also been carried out. Additionally, a comparative docking study for potential selectivity and binding orientation of these novel prodrugs into the binding sites of COX-1 and COX-2 enzyme was also carried out.Compound **1** showed considerable more binding affinity for COX-1 enzyme in comparison to COX-2.

Keywords: Steroid-NSAID prodrug, MEP, NLO, DFT, NBO, Molecular docking

1. Introduction

Diosgenin, a precursor of steroid hormones is an important biologically active compound which controls hyper-cholesterolemia by improving the lipid profile as well as modulating oxidative stress [1]. Diosgenin has also possesses antioxidant and anti-apoptotic activities[2].

Another biologically significant steroid 16–dehydropregnenalone acetate, best prepared from diosgenin or solasodine [3] finds increasing application as a versatile scaffold and building block for different steroidal pharmacophores including anti–fertility and anti–inflammatory drugs [4].NSAIDs are the drugs most widely used for getting relief from acute and chronic pain. However, their frequent use is associated with a broad spectrum of adverse effects, related to inhibiting prostaglandin synthesis in tissues where PG's are responsible for physiological homeostasis [5]. As most NSAIDs posses a carboxyl group, hence one of the strategy adopted to avoid gastrointestinal (GI) damage involves carrying out the esterification of the NSAID. It has been reported that esterification of the carboxylic acid moiety of NSAIDs suppress gastro-toxicity without adversely affecting their anti-inflammatory activity [6, 7]. Continuing in our effort towards synthesis of some novel steroid-NSAIDs prodrugs [8, 9], based on esterification of our biologically active steroids with the standard anti–inflammatory drug naproxen, two new prodrugs 3β–2–(6–methoxynapthalen–2–yl)–propioxy–5β–spirost–5–en(**1**)and20–oxo–pregn–5,16–diene–3β–yl–2–(6–methoxynapthalen–2–yl) propionate (**4**) were synthesized. Synthesized prodrugs are represented in **Scheme 1**. A comparative docking study of these newly synthesized compounds into the active sites of COX–1 and COX–2 enzymes was studied. Most of the NSAIDs inhibit both COX–1 and COX–2 enzymes with little specificity leading to serious side effects such as gastric lesions and renal toxicity [10].

The structures of newly synthesized ester derivatives have been interpreted with the help of ¹H, ¹³C NMR, IR, UV-Visible spectroscopy and mass spectrometry. Density Functional Theory (DFT) with the help of B3LYP functional and 6-31G (d, p) basis set was used for optimizing the geometry of newly synthesized derivatives.

Vibrational frequency of compound **1** and **4** have also been calculated by using these basis set. The results were compared with the experimental observations. Further, nuclear magnetic chemical shifts have been calculated with the same functional and basis set using GIAO method and result have been compared with the experimental data. HOMO-LUMO analysis was also carried out to predict various transitions using time dependent TD-DFT approach. AIM approach has extensively been applied to understand hydrogen bonding interactions and ellipticity in the synthesized molecules.

The present paper aims to give a complete description of chemical shifts, vibrational assignments, intramolecular interactions, electronic transitions, global reactivity descriptors, molecular electrostatic potential and NLO and molecular docking of the synthesized compounds.
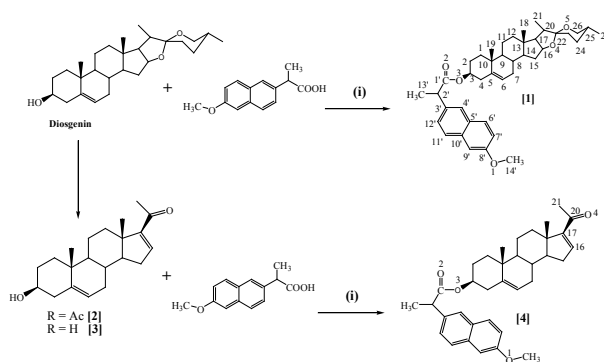
Scheme 1: (i)DCC/DMAP, stirrer at room temp.

2. Experimental

2.1.Materials and measurements

All commercially available solvents and reagents were of analytical grade and were used without further purification. ¹H nuclear magnetic resonance (NMR) was recorded on Bruker DRX–300 MHz and JOEL AL 300 FTNMR and ¹³C NMR were recorded on JOEL

AL 300 FTNMR (75Mz) using TMS as an internal reference. IR spectra were recorded on Perkin Elmer FTIR spectrometer from 4000–400 cm^{-1} range. The spectra were analyzed using Spectrum™ Software suite. ESI–MS spectra were recorded on **Agilent 6520 Q–TOF mass spectrometer.Elemental analysis was carried out on Perkin Elmer 2400 CHN elemental analyzer.**

2.2.3β–2–(6–methoxynapthalen–2–yl)–propioxy–5β–spirost–5–en (1)

A solution of 2–(6–methoxynapthalen–2–yl) propionic acid (278 mg, 1.2mmol), DCC (312 mg, 1.5mmol), DMAP (2.46 mg, 0.02mmol) and diosgenin (420 mg, 1.01mmol) in chloroform (25 mL) were stirred mechanically at room temperature for 2 h until reaction was complete (progress of reaction was monitored by TLC). *N,N*–dicyclohexylurea (DCU) formed during the reaction was filtered off and the filtrate washed successively with 5% NaCl solution, saturated NaHCO$_3$ solution, water and then dried over anhydrous sodium sulfate. Chloroform was evaporated under reduced pressure and the crude product obtained was purified by column chromatography using ethyl acetate–hexane (2:98) as eluent to obtain compound **1** (357 mg, 85% yield) m.p. 222°C. ^{1}H NMR(CDCl$_3$,300 MHz) δ(ppm) 7.71 (1H, d, H–6', J=2.4Hz), 7.69 (1H, d, H–11', J=2.3Hz), 7.66 (1H, s, H–4'), 7.42 (1H, dd, H–12', J=1.2 & 7.2Hz), 7.15 (1H, d, H–7', J=2.4Hz), 7.11 (1H, s, H–9'), 5.30 (1H, d, H–6, J=3.9Hz), 4.70–4.58 (1H, m, H–3), 4.40 (1H, q, H–16, J=7.5Hz), 3.91 (3H, s, CH$_3$–14'), 3.82 (1H, q, H–2', J=6.9Hz), 3.47–3.45 (1H, m, H–26e), 3.36 (1H, t, H–26a, J=10.8Hz), 1.66–1.59 (1H, m, H–25), 1.56 (3H, d, CH$_3$–13', J=7.2Hz), 0.95 (3H, d, CH$_3$–21, J= 6.9Hz), 0.98 (3H, s, CH$_3$–19), 0.79 (3H, d, CH$_3$–27, J=7.2Hz), 0.77 (3H, s, CH$_3$–18);^{13}C NMR (75MHz,CDCl$_3$) δ (ppm) 174.0 (C–1',C=O), 157.5 (C–8'), 139.5 (C–5), 135.9 (C–3'), 133.5 (C–10'), 129.2 (C–5'), 128.8 (C–6'), 127.0 (C–

12'), 126.2 (C–4'), 125.8 (C–11'), 122.2 (C–6), 118.8 (C–7'), 109.2 (C–22), 105.5 (C–9'), 80.7 (C–16), 74.1 (C–3), 66.8 (C–26), 62.0 (C–17), 56.3 (C–14'), 49.8 (C–9), 45.6 (C–14), 41.5 (C–20), 40.2 (C–2'), 39.6 (C–13), 37.7 (C–12), 36.9 (C–4), 36.6 (C–10), 31.9 (C–1), 31.7 (C–15), 31.3 (C–8), 30.2 (C–7), 29.6 (C–23), 28.7 (C–25), 27.6 (C–24), 24.6 (C–2), 20.7 (C–11), 19.3 (C–19), 18.6 (C–18), 17.1 (C–27), 16.2 (C–21), 14.5 (C–13');MS m/z =626 [M$^+$, not observed], 437 [M$^+$–139–CH$_3$OH–H$_2$O], 312 [512–C$_{13}$H$_{14}$O–CH$_3$].Anal. Calc. for C$_{41}$H$_{54}$O$_5$: C, 78.55; H, 8.68. Found: C, 77.58; H, 8.36.

2.3.20–oxo–pregn–5,16–diene–3β–yl–2–(6–methoxynapthalen–2–yl)propanoate (4)

A solution containing 3β–hydroxy–pregn–5,16–diene–20–one (**3**) (314 mg, 1mmol), 2–(6–methoxynapthalen–2–yl) propionic acid (230 mg, 1mmol), DCC (315 mg, 1.5mmol), DMAP (2.5 mg, 0.02mmol) in chloroform (25 mL) was stirred for 3 h at room temperature. Workup procedure was similar as given in synthesis of **1**. The crude product was purified by column chromatography on silica gel (ethyl acetate–hexane 2:98) to yield compound **4** (219.8 mg, 70% yield) m.p. 238°C. ^{1}H NMR(CDCl$_3$,300 MHz) δ(ppm)7.70–7.68 (3H, m, H–4', H–6', H–11'), 7.42 (1H, m, H–12'), 7.11 (2H, m, H–7' and H–9'), 6.69 (1H, m, H–16), 5.31 (1H, m, H–6), 4.75 (1H, m, H–3), 3.91 (3H, s, CH$_3$–14'), 3.82 (1H, m, H–2'), 2.25 (3H, s, CH$_3$–21), 1.56 (3H, d, CH$_3$–13', J=3.3Hz), 1.02 (3H, s, CH$_3$–19), 0.90 (3H, s, CH$_3$–18);^{13}C NMR (75MHz,CDCl$_3$) δ (ppm) 196.8 (C–20,C=O), 174.0 (C–1', C=O), 157.5 (C–8'), 155.3 (C–17), 144.4 (C–16), 140.1 (C–5), 135.9 (C–3'), 133.5 (C–10'), 129.2 (C–5'), 128.9 (C–6'), 127.0 (C–12'), 126.2 (C–4'), 125.8 (C–11'), 121.9 (C–6), 118.8 (C–7'), 105.5 (C–9'), 74.08 (C–3), 56.3 (C–14'), 55.3 (C–9), 50.30 (C–14), 46.0 (C–13), 45.6 (C–2'), 37.8 (C–4), 36.8 (C–1), 36.7 (C–10), 34.5 (C–12), 32.2 (C–15), 31.4 (C–7), 30.0 (C–8), 27.6 (C–

2), 27.1 (C–21), 20.5 (C–11), 19.2 (C–19), 18.6 (C–18), 15.6 (C–13');MS m/z =526 [M$^+$, not observed], 549 [526+Na]$^+$, 437 [M$^+$–COCH$_3$–CH$_3$–OCH$_3$], 298 [M$^+$–C$_{13}$H$_{13}$O–COCH$_3$], Anal. Calc. for C$_{35}$H$_{42}$O$_4$: C, 79.81; H, 8.03. Found: C, 79.32; H, 8.86.

3. Computational study

The entire calculations were performed at density functional theory (DFT) level using Gaussian 09W [11] program package and Gauss view [12] visualization program, invoking gradient geometry optimization. The optimized structural parameters were used in the vibrational frequency calculations at DFT level to characterize all stationary points as minima. ^{1}H and ^{13}C NMR chemical shifts were calculated with GIAO approach [13]. UV–Vis spectra, electronic transitions, vertical excitation energies and electronic properties such as HOMO and LUMO energies were determined with time–dependent DFT (TD–DFT) approach. Potential energy distribution (PED) along with internal coordinates was calculated by Gar2ped software [14].

4. Molecular Docking study

Molecular docking is a method to predict the preferred orientation of one molecule with respect to the second when bound to each other to form a stable complex. It evaluates how well a molecule (like a substrate, inhibitor, or a drug candidate) fits well within the active site of the target macromolecule (like receptor, enzyme or nucleic acid). The study is useful for developing better drug candidates and for understanding the nature of binding. We carried out acomparative COX–1 and COX–2 docking study of two new steroidal prodrugs with the aim to discuss the possible interactions of these ligands into the crystal structure of COX–1 and COX–2 enzymes. The three dimensional structure of enzymes COX–1 (PDB 3N8Z) and COX–2

(PDB 3NT1) were obtained from Protein Data Bank (http://www.rcsb.org/pdb/home/home. do).Docking calculations were performed with program LibDock implemented in Discovery studio 3.5(DS 3.5, Accelrys Software Inc.; San Diego; http://www.accelrys.com).

5. Result and Discussion

5.1. Vibrational spectral analysis

The observed FT–IR frequencies for various modes of vibrations and descriptions concerning the assignments for compound **1** and **4** are presented in **SupplementaryTable 1S** and **2S**respectively along with the corresponding harmonic–vibrational frequencies calculated at B3LYP/6–31G (d,p) level. The calculated harmonic frequencies were scaled down via scaling factor 0.9608 [15].

In case of compound**1**, the FT–IR bands observed at 3058cm^{-1}for C-H stretching of aromatic, C–H stretching vibrations for methyls and methylenes at 2929 cm^{-1}, 2906 cm^{-1}, 2856 cm^{-1}. The asymmetric and symmetric bending of CH$_3$-18 observed at 1482 and 1377cm^{-1} respectively. A strong band observed at 1720 cm^{-1} was assigned to the C=O stretching vibration for ester group and band observed at 1652 cm^{-1} corresponds to the C=O stretching vibration for the conjugated ketone at C-20. The aromatic ring stretching vibrations (C=C–C) were observed at 1604 cm^{-1}and1529 cm^{-1}.

In FT–IR of**4**, aromatic C-H stretching vibration at 3050cm^{-1}whereasaromatic ring stretching vibrations (C=C–C) were observed at 1629 cm^{-1},1603.8 cm^{-1}, 1504.6 cm^{-1}, 1482.5 cm^{-1}. The C–H stretching vibrations for methyls and methylenes at 2963.8 cm^{-1}, 2936.8 cm^{-1}, 2851.2 cm^{-1}. The CH$_2$ scissoring band is observed at 1430.4 cm^{-1}. The CH$_2$waging and twisting vibrations are observed at 1267 and 1228 cm^{-1}respectively. A strong band observed at

1720.7 cm^{-1} was assigned to the C=O stretching vibration for ester group and the stretching vibration for the α, β-unsaturated ketone (C=O) at C-20 was observed at 1670.4 cm^{-1}.

5.2. NMR spectral analysis

Selected theoretical and experimental chemical shifts of both compound **1** and **4** in ^{1}H and ^{13}C NMR spectra are shown in **Table 1**. In the ^{1}H NMR spectrum of compound **1** the appearance of signals for aromatic ring protons at δ 7.71 (H–6', J=2.4Hz), 7.69 (H–11', J=2.3Hz), 7.66 (H–4'), 7.42 (H–12', J=1.2 & 7.2Hz), 7.15 (H–7',J=2.4Hz), 7.11 (H–9') together with a three proton singlet at δ 3.91 for H–14' (CH$_3$ of methoxy group) , a one proton quartet at δ 3.82 (J=6.9Hz) for H–2', three proton doublet at δ 1.56 (J=7.2Hz) for CH$_3$–13' methyl group, along with the downfield shifting of H–3 methine proton now appearing as a multiplet at δ 4.70–4.58 suggested the esterification of the C-3 hydroxyl group of diosgenin. In the ^{13}C NMR spectrum of compound **1** the appearance of carbon signal at δ 174.0 corresponding to esterified carbonyl carbon with aromatic carbons at 157.5 (C–8'), 135.9 (C–3'), 133.5 (C–10'), 129.2 (C–5'), 128.8 (C–6'), 127.0 (C–12'), 126.2 (C–4'), 125.8 (C–11'), 118.8 (C–7') and 105.5 (C–9') along with C–3 carbon appearing at δ 74.1 confirmed the esterified nature of C–3 hydroxyl group. These observed chemical shifts for both ^{1}H and ^{13}C NMR for **1** showed good relationship with the calculated results.

^{1}H NMR spectrum of compound **4**,shows the downfield signals observed at δ 7.70–7.68 (H–4', H–6', H–11'), 7.42 (H–12'), 7.11 (H–7', H–9') for aromatic ring protons along with a three proton singlet at δ 3.91 for H–14' (CH$_3$ of methoxy group) , a three proton doublet at δ 1.56 (J= 3.3Hz) for CH$_3$–13' methyl group and a one proton multiplet at δ 3.82 for H–2' together with the downfield shifting of H–3 methine proton observed as a multiplet at δ 4.75 suggested the

esterification of C–3 hydroxyl group. In the ^{13}C NMR spectrum, the esterification by aromatic moiety was confirmed by the presence of signal for the carbonyl carbon of ester at δ174.0 along with the signals for the aromatic carbons at 157.5 (C–8'), 135.9 (C–3'), 133.5 (C–10'), 129.2 (C–5'), 128.9 (C–6'), 127.0 (C–12'), 126.2 (C–4'), 125.8 (C–11'), 118.8 (C–7'), 105.5 (C–9') respectively.

5.3. Electronic properties

The experimental absorption wavelength (λ), excitation energies (E), Oscillator strength (*f*), major contributions of the transitions and assignments of electronic transitions for compounds **1** and **4** are tabulated in **Table 2**. According to TD–DFT approach, the maximum absorption wavelength in case of calculated electronic absorption spectra corresponds to the electronic transition from highest occupied molecular orbital (HOMO) to the lowest unoccupied molecular orbital (LUMO). The energy gap between the HOMO and LUMO is a critical parameter in determining molecular electrical transport properties because it is a measure of electron conductivity [16]. **Fig. 1a** and **1b** shows thedistribution and corresponding energy of the Frontier molecular orbitals computed at B3LYP/6–31G (d,p) level for compounds **1** and **4.** The absorption wavelengths for compound **1** were observed at 236 nm and 220 nm. Similarly, the absorption wavelengths for compound **4** were observed at 243 nm and 219 nm respectively. For compound **1,** the experimental band at 236 nm is attributed mainly to H→L+1 transition with 80.4 % contribution and the band at 220 nm is attributed mainly to H–6→L transition with 68.4% contribution. Similarly, for compound **4** the experimental band at 243 nm is attributed mainly to H–1→L+1 transition with 79.5 % contribution and the band at 219 nm is attributed mainly to H→L+3 transition with 76.9 % and H→L+2 transitions with 94.2 % contribution.

All the transitions were predicted as $\pi \rightarrow \pi^*$.

5.4. Natural Bond order analysis (NBO)

NBO analysis has an appealing aspect of highlighting the individual bonds and lone–pair energy that play a vital role in the chemical processes [17–19]. It is an important tool for studying hybridization, covalency, hydrogen–bonding and Van der Waals interactions [20, 21]. In other words natural bond orbital (NBO) provides supplementary structural information. Second–order perturbation theory analysis of the Fock matrix in NBO basis for compounds **1** and **4** are presented in **Supplementary Table 3S** and **4S**. In compound **1** some of the important $\pi \rightarrow \pi^*$ interactions viz. π (C3'–C4') $\rightarrow$ π^*(C12'–C11')/ π^*(C5'–C10'); π(C12'–C11') $\rightarrow$ π^*(C3'–C4')/ π^*(C5'–C10'); π (C5'–C10') $\rightarrow$ π^*(C3'–C4')/ π^*(C12'–C11')/ π^*(C6'–C7')/ π^*(C9'–C8'); π(C6'–C7') $\rightarrow$ π^*(C5'–C10')/ π^*(C9'–C8'); π(C9'–C8') $\rightarrow$ π^*(C5'–C10')/ π^*(C6'–C7') are responsible for the delocalization of respective π–electrons of naphthalene ring due to high electron density at π bonds (1.735–1.773) and low density at π^* bonds (0.254–0.415) and the molecule being stabilized by energy in the region of 15.96~18.20 kJ/mol. The n_2 (O1) $\rightarrow$$\pi^*$(C9'–C8') interaction indicate the involvement of lone pair of electrons on the oxygen atom of methoxy group with π–electron delocalization in naphthalene ring with 31.77 KJ/mol energy stabilization.

Similarly in compound **4**, the delocalization of the π–electrons along with the involvement of lone–pair of electrons on the oxygen atom of methoxy group was also studied. The different interactions responsible for the delocalization of respective π–bonds in naphthalene ring aresummarized as π(C3'–C4') $\rightarrow$ π^*(C12'–C11')/ π^*(C5'–C10'); π(C12'–C11') $\rightarrow$ π^*(C3'–C4')/ π^*(C5'–C10'); π(C5'–C10') $\rightarrow$ π^*(C3'–C4')/ π^*(C12'–C11')/ π^*(C6'–C7')/ π^*(C9'–C8'); π(C6'–C7') $\rightarrow$ π^*(C5'–C10')/

π^*(C9'–C8'); π(C9'–C8') $\rightarrow$ π^*(C5'–C10')/ π^*(C6'–C7') show high electron density at π bonds (1.653–1.962) and low electron density at π^* bonds (0.2540–0.415). These interactions stabilize the molecule with energy in the region 17.45~71.18 kJ/mol. Other high energy interactions involving the lone pair of electrons with the π electrons corresponds to n_2 (O3) $\rightarrow$ π^*(C1'–O2) and n_2 (O1) $\rightarrow$ π *(C9'–C8') stabilizing the molecule with 51.07 kJ/mol and 31.81 kJ/mol energy respectively. In compound **4** another important donor acceptor contact occurs π (C17–C16) $\rightarrow$ π^*(O4–C20) and π (O4–C20) $\rightarrow$ π^*(C17–C16) responsible for the conjugation of respective C16-C17 π–bond with the lone pair of electrons on C-20 carbonyl oxygen atom which stabilized the molecule with a maximum energy ~20.61 kJ/mol. At last it can be conclude that all these interactions stabilized both the molecules.

5.5. Molecular Electrostatic Potential

Molecular electrostatic potential surface (MEP) for all the compounds were calculated by DFT/B3LYP at 6-31G (d, p) basis set and MEP surface are plotted in **Fig. 2**. It simultaneously displays the molecular shape, size, and charge distribution, as well as reactive sites of a molecule. The red and yellow regions of the MEP are related to electrophilicreactivity and the blue regions to nucleophilic reactivity. It is clear that in compound Diosgenineand**3**,oxygen atom (redregion) of hydroxyl group at C-3is a good nucleophile and they reacts with naproxen to form ester **1** and **4**.

5.6. Global reactivity descriptors

The chemical reactivity of the molecular systems has been determined by the conceptual density functional theory [22].Electronegativity (χ), chemical potential (μ), global hardness (η), global softness (S) and electrophilicity index (ω)are global reactivity descriptors,

highly successful in predictingglobal reactivity trends. On the basis of Koopmans's theorem, [23] global reactivity descriptors are calculated using the energies offrontier molecular orbitals ε_{HOMO}, ε_{LUMO} as

$$\chi = -1/2(\varepsilon_{LUMO} + \varepsilon_{HOMO})$$

$$\mu = -\chi = 1/2(\varepsilon_{LUMO} + \varepsilon_{HOMO}),$$

$$\eta = 1/2(\varepsilon_{LUMO} - \varepsilon_{HOMO}), \quad S = 1/2\eta \quad \text{and}$$

$\omega = \mu^2/2\eta$. The energies of frontier molecular orbitals (ε_{HOMO}, ε_{LUMO}) and global reactivity descriptors for **1**and**4** are listed in **Table 3**.The frontier orbital gap helps to characterize molecular electrical transport properties, the chemical reactivity and kinetic stability of the molecule[24, 25]. A molecule with a small frontier orbital gap is generally associated with a high chemical reactivity and low kinetic stability. The frontier orbital energy gap for both the compounds was found to be 4.622eV and 4.333eV respectively. Larger the HOMO-LUMO energy gap, harder the molecule. The HOMO–LUMO energy gap of compound **1** was slightly larger, signifying higher excitation energy in comparison to **4**, hence compound **1** is harder in comparison to compound **4**. When two molecules react, which one will act as an electrophile or nucleophile will depend upon the value of electrophilicity index. Higher the value of the electrophilicity index better is the electrophilic character. Thus, between compound **1** and **4**, compound **4** acts as a good electrophile as the molecule shows higher value for global electrophilicity index (ω) at 2.645 eV, as compared to compound **1** whose values for global electrophilicity index (ω) was 2.209 eV.

5.7. AIM approach

In the topological theory of AIM (atom in molecule), when two neighboring atoms are chemically bonded, a bond critical point appears between them and the nature of chemical bonds and molecular reactivity are described by total electronic density, $\rho(r)$, and its corresponding Laplacian, $\nabla^2\rho(r)$. Laplacian of total electronic density is related to energetic topological parameters by a local expression of the virial theorem at critical points [26]:

$$\frac{1}{4}\nabla^2\rho(r) = 2G(r) + V(r)$$

Where, $G(r)$ and $V(r)$ are the kinetic and potential electron energy densities at critical points respectively. As Rozas*et al.*[27] explained; hydrogen bonds can be classified as (1) Weak hydrogen bonds $\nabla^2\rho(rBCP) > 0$ and $G(rBCP) + V(rBCP) > 0$; (2) Medium hydrogen bonds $\nabla^2\rho(rBCP) > 0$ and $G(rBCP) + V(rBCP) < 0$; (3) Strong hydrogen bonds $\nabla^2\rho(rBCP) < 0$ and $G(rBCP) + V(rBCP) < 0$; Where $G(rBCP)+V(rBCP)$ is also known as total electron energy density, $H(rBCP)$. The typical ranges of $\rho(r)$ and $\nabla^2\rho(r)$ for hydrogen bond in BCP are 0.002–0.035e/a3°and 0.02–0.139e/a5°, respectively [28].Several theoretical methods [29, 30]have been proposed to estimate hydrogen bond energy. One of the most useful of these methods has been explained by Espinosa *et al.*[31]who found that IHB energy may be correlated with the potential electron energy density at critical point by the expression $E_{IHB} = 1/2V(rBCP)$.Molecular graph of the synthesized compounds using AIM program at B3LYP/6- 31G (d, p) level are shown in **Fig. 3**.For compounds **1** and **4**topological parameters for bonds of interacting atoms are given in **Table 5S (Supplementary material)** andon the basis of above criteria $\nabla^2\rho(rBCP)$ and H_{BCP} parameters are greater than zero suggested all the interactions are weak.According to AIM calculation, the total energy of intramolecular interaction for compound **1** and **4**was calculated as -10.94 and-7.81 kcal/mol respectively. The ellipticity (ε) at BCP is a sensitive index to monitor the π-character of bond. The ε is related to λ_1 and λ_2, which correspond to the eigen values of Hessian and defined by a relationship: $\varepsilon = (\lambda_1/\lambda_2) - 1$. The ellipticity values for bonds C3′ – C4′, C4′ – C5′, C5′ – C6′, C6′ – C7′, C7′– C8′, C8′ – C9′,C9′ – C10′, C10′ – C11′, C11′– C12′, C12′ – C3′ andC10′ – C5′in compound **1**are

0.261, 0.170, 0.157, 0.273, 0.198, 0.305, 0.173, 0.163, 0.257, 0.170 and 0.155 respectively. The ellipticity values of compound **4** are similar as mention for **1**. The lower values of ellipticity confirm that there is delocalization of electron in aromatic ring [32].

5.8. NLO analysis

Molecules with second-order nonlinear optical (NLO) property have received much attention in the recent years as they have found vast applications in the optoelectronic devices of telecommunications, optical fibres, information storage, optical switching, and signal processing [33-36]. Therefore a theoretical investigation of the NLO properties of synthesized derivatives by means of density functional theory (DFT) was carried out.The first order hyperpolarizability (β_o) of compounds **1** and **4** and related properties (μ_o, $|\alpha_o|$) were calculated using B3LYP/6-31G (d, p) basis set. Calculated dipole moment (μ) polarizability ($|\alpha_o|$) and hyperpolarizability (β_o) by NLO is given in **Table 4**.

First order hyperpolarizability (β_o)for both the compounds was calculated by taking into account the Kleimman symmetry relations and the square norm of the Cartesian expression for the βtensor [37, 38]. The total static dipole moment μ_o, mean polarizability ($|\alpha_o|$) and the mean first hyperpolarizability β_o, using the x, y, z components are defined as

$$\mu_0 = (\mu_X^2 + \mu_Y^2 + \mu_Z^2)^{1/2}$$

$$|\alpha_0| = 1/3\,(\alpha_{xx} + \alpha_{yy} + \alpha_{zz})$$

$$\beta_0 = [(\beta_{xxx} + \beta_{xyy} + \beta_{xzz})^2 + (\beta_{yyy} + \beta_{xxy} + \beta_{yzz})^2 + (\beta_{zzz} + \beta_{xxz} + \beta_{yyz})^2]^{1/2}$$

Since the value of the polarizability ($|\alpha_0|$), first hyperpolarizability (β_o) of Gaussian 09 output are reported in atomic unit (a.u.) thus these values are converted into electrostatic unit (esu) using converting factors as (for ($|\alpha_0|$): 1 a.u. = 0.1482×10^{-24}esu; for β_o: 1 a.u = 0.008639×10^{-30} esu). The calculated values of (β_o)for compounds

1 and **4** were 6.565×10^{-30}esuand 8.035×10^{-30}esurespectively which was greater than those of urea (the $\beta_o$of urea 0.3728×10^{-30}esu). Theoretically, the first hyperpolarizability of the compound **1** is 17 times and compound **4** is nearly 21 times greater than that of urea. Hence it is concluded that both the compounds may act as good NLO material and show optical properties. Besides in comparisonto **1**, compound **4**may be a better applicant in the development of NLO materials.

5.9. Molecular docking

Molecular docking is a well established computational technique which predicts the interaction energy between two molecules and is frequently used for understanding drug–receptor interaction. In the present study, acomparative COX–1 and COX–2 docking study was done to explain the possible interaction of compounds**1** and **4** into the crystal structure of COX–1 and COX–2 enzymes. Docking results have been explained taking into account the parameters like hydrogen bonding and non polar Pi–cation (non–covalent) interactions. The strength of cation–π interaction were investigated theoretically by Gallivan and Dougherty [39] and it was inferred that these interactions were potentially more stabilizing than hydrogen bonding or salt bridges and play an important role in defining the molecular recognition and interaction with ligands. The orientation and binding affinity of 2–arylpropionic acid moiety present in NSAIDs has been extensively studied [40]. Naproxen one of the potent NSAIDs, inhibit the activity of both COX–1 and COX–2 enzyme and this inhibition is probably due to hydrogen bonding between the COOH group of naproxen and the amino acid residues Arg120 and Tyr 355 present at the base of the active site in COX-enzymes [40]. The other contacts that occur between the drug naproxen and protein correspond to different types of Van der Waals interactions including pi interactions. In the present study

a comparative COX–1 and COX–2 docking was carried out with newly synthesized steroid-NSAIDs prodrugs **1** and **4**. It was observed that both **1** and **4** interacted with COX–1 and COX–2 in a manner similar to standard drug naproxen, by making use of hydrogen bonds and pi–cation monitor although no pi–pi interactions were observed (**Fig. 4**). The details of such interactions generated between **1** and **4** with COX–1 and COX–2 enzyme are best illustrated in **Table 6S**(**Supplementary material**). In case of molecular docking of **1** and **4** with COX–1 receptor, one hydrogen bond was observed between amino acid ARG120:HH21 (2.37Å) and O17 (O2 of **1** as in **Scheme 1**) carbonyl oxygen for **1** (**Fig. 4a**) and two hydrogen bonding interactions were seen involving amino acid residues ARG120:HE(1.91Å) and ARG120:HH21(2.01Å) with O16 (O2 of **4** as in **Scheme 1**) carbonyl oxygen in case of **4** (**Fig. 4b**) respectively. In addition to hydrogen bonds, two pi–cation interactions each for **1** and **4** were also seen using the naphthyl ring of naproxen and GLY526N (6.12Å, 6.25Å) and ILE523N (5.81Å, 6.83Å) amino acid residues of COX–1 enzyme respectively (**Table 6S**). In a similar fashion, the molecular docking study involving **1** and **4** with COX–2 receptor was undertaken and it was seen that **1** formed two types of hydrogen bonds between ARG120:HE and O17 (O2 of **1** as in **Scheme 1**) (1.97 Å) and between ARG120:HH21 and O16 (O3 of **1** as in **Scheme 1**) (2.48 Å) (**Fig. 4c**). It also displayed pi–cation interaction between GLY526:N and the aromatic ring with interatomic distance of 4.45 Å. On the other hand, **4** displayed two hydrogen bonding interactions between ARG120:HE and O16 (O2 of **4** as in **Scheme 1**) atom of ester function (1.83 Å) and ARG120:HH21 and O17 atom respectively (O3 of **4** as in **Scheme 1**) (**Fig. 4d**). One pi–cation interaction involving A: ARG120:NH$_2$ with the naphthyl ring of naproxen was also observed with interatomic distance of 5.43 Å. From post docked poses obtained after docking of **1** and **4**, it was

inferred that the molecules under question were deeply buried and stabilized into the active site of both COX–1 and COX–2 receptor through hydrogen bonds and pi–cation interactions. For both the molecules (**1** and **4**) protein residue ARG120 was responsible for hydrogen bonding and GLY526 and ILE523 for pi–cation interactions. The cyclooxygenase inhibitory activity of the **1** and **4** were compared with the standard drug naproxen. The binding affinity of **1** and **4** were evaluated and compared with the standard drug naproxen on the basis of binding energies (Kcal/mol) and Libdock score **Table 7S**(**Supplementary material**). The lower the binding energy and higher the Libdock score, better the binding affinity. Prodrug **1** exhibited greater binding affinity for COX-1 enzyme with binding energy (−107.3Kcal/mol) lower than that of the standard drug naproxen (−101.9Kcal/mol) and the corresponding value of Libdock score was higher in case of **1** (94.12) when compared to the standard drug naproxen (89.63). Further, docking result of compound **4** with COX-1 showed poor binding affinity with low value of negative binding energy (−34.57Kcal/mol). Similar set of observations were made for molecular docking of **1** and **4** with COX-2 receptor, where the binding affinity of **1** and **4** were comparable to that of the standard drug (**Table 7S**). The important pharmacophore feature responsible for the hydrogen bond formation in **1** and **4** is the ester function which acts as hydrogen bond acceptor. Thus the aforementioned docking results indicate that **1** could be a better substrate for COX–1 inhibition and in turn a better candidate for the treatment of inflammation in comparison to standard drug naproxen. The results are encouraging and in order to improve our knowledge in understanding the binding interactions for such type of compounds in detail and for development of potent cyclooxygenase inhibitors, there is a need to carry out esterification of the carboxylate moiety of the anti-inflammatory drugs with a more 'suitable' steroidal moiety.

6. Conclusion

Limitations of most NSAIDs due to gastric damage caused by the free carboxyl group led us to synthesize two new Steroid-NSAIDs prodrugs in good yield. The structures were characterized with the help of ^{1}H, ^{13}C NMR, FT-IR, UV and mass spectrometry.A combined molecular orbital coefficients analysis and molecular orbital plots suggested the nature of electronic excitations of both the compounds to be $\pi \rightarrow \pi^*$. From global reactivity descriptors **4** can act as a good electrophile as the molecule shows high values for global electrophilicity index (2.645eV). On the basis of first hyperpolarizability, we conclude that investigated molecules will show non-linear optical response and may be used as non-linear optical material. Ester derivatives have been stabilized by weak intramolecular interactions, proof with the help of AIM approach. A comparative COX-1 and COX-2 molecular docking study of the synthesized compounds was carried out and it was observedthat binding affinity of compound **1** withCOX-1 was more in comparison to binding affinity of parent drug naproxen with COX-1.Therefore it can be concluded that compound **1**, which is a better inhibitor of target enzyme could prove to be a better anti-inflammatory drug.

Acknowledgement

Supplementary material

The FT-IR, ^{1}H NMR, ^{13}C NMR spectra and of compound **1** and **4** are given inSupplementary material**.**

References

1. A. Sethi, A. Bhatia, G. Bhatia, A. Srivastava, R. Prakash, J. Mol. Str., 1052 (2013) 76–84.
2. Chih-Tai Chen, et al., Nutrients 7 (2015) 4938-4954.
3. A. Sethi, A. Maurya, V. Tewari, S. Srivastava, S. Faridi, G. Bhatia, M. M. Khan, A. K. Khanna, J. K. Saxena, Bioorg. Med. Chem., 15 (2007) 4520–4527.
4. M. Cabeza, I. Heuze, E. Bratoeff, E. Ramirez, R. Martinez, Chem. Pharm. Bull. 49 (2001) 525–530.
5. G. Coruzzi, N. S. Venturi, S. Spaggiari, Acta Bio. Med., 78 (2007) 96–110.
6. J. R. Laporte, X. Carne, X. Vidal, V. Mareno, J. Juan, Lancet, 337 (1991) 85–89.
7. N. Weber, P. Weitkamp, K.D. Mukherjee, Food. Res. Int. 35 (2002) 177.
8. A. Sethi, G. Bhatia, A. K. Khanna, M. M. Khan, A. Bishnoi, A. K. Pandey, A. Maurya, Med. Chem. Res., 20(2011) 36–46.
9. A. Sethi, A. Bhatia, A. Maurya, A. Panday, G. Bhatia, A. Shrivastava, R. P. Singh, R. Prakash, J. of Mol. Str., 1052 (2013) 76–84.
10. I. L. Meek, M. A.F.J. van de Laar, H. E. Vonkeman, Pharmaceuticals (Basel). 3(7), (2010), 2146–2162.
11. M.J. Frisch et al. Gaussian 09, Revision A.1, Gaussian, Inc., Wallingford CT, 2009.
12. Gauss View 5.09 program Gaussian, Inc., Wallingford, CT, 06492 USA.
13. K. Wolinski, J. F. Hinton, P. Pulay, J. Am. Chem. Soc., 112 (1990)8251–8260.
14. J. M. L. Martin, V. Alsenoy, C. V. Alsenoy, Gar2ped, University of Antwerp,1995.
15. N. Sundaraganesan, E. Kavitha, S. Sebastian, J. P. Cornard, M. Martel, Spectrochim. Acta Part A., 74 (2009) 788–797.
16. J. Fleming, Frontier Orbitals and Organic Chemical Reactions, 249 S, Wiley, London, 1976.
17. V. Pophristic, L. Goodman, N. Guchhait, J. Phy. Chem., 101 (1997) 4290–4297.
18. D. Geo, L. Goodman, J. Phys. Chem., 100 (1996) 12540–12545.
19. F. Weinhold, Nature, 411 (2001)539–541.
20. J. P Foster, F. Weinhold, Natural hybrid orbitals. J. Am. Chem. Soc. 102 (1980) 7211–7218.
21. F. Weinhold, C. R. Landis, Valency and Bonding: A Natural Bond Orbital Donor–Acceptor Perspective, Cambridge University Press, Cambridge, New York, Melbourr, 2005, 215–274.
22. R.G. Parr and W. Yang, Density Functional Theory of Atoms and Molecules, Oxford University Press, Oxford, New York, 1989.
23. T. Koopmans, Physica. 1 (1934) 104-113.
24. A. Sethi, R. P. Singh et al., J. Mol. Struct. 1130 (2017) 860-866.
25. K Fukui. Science. 218 (1982) 747–754.

26. R. F. W. Bader, Atoms in Molecules, A Quantum Theory, Oxford University Press, Oxford, 1990.

27. I. Rozas, I. Alkorta, J. Elguero, J. Am. Chem. Soc. 122 (2000) 11154-11161.

28. Shainyan B A, Chipanina N N, Aksamentova T N, Oznobikhina L P, Rosentsveig G N and Rosentsveig I B 2010 Tetrahedron 66 8551.

29. Schuster P, Zundel G and Sandrafy C 1976. The hydrogen bond (Amsterdam: North Holland Publ. Co.).

30. Nowroozi A, Raissi H and Farzad F.,J. Mol. Struct. (THEOCHEM) 730 (2005)161.

31. Espinosa E, Molins E and Lecomte C.,Chem. Phys. Lett. 285 (1998)170.

32. R. P. Singh, A. Sethi et al., J. Mol. Struc. 1095 (2015) 125-134.

33. D. Sajan, H. Joe, V.S. Jayakumar, J. Zaleski, J. Mol. Struct. 785 (2006) 43.

34. C.Andraud, T.Brotin, C.Garcia, F.Pelle, P.Goldner, B.Bigot and A. Collet. J. Am. Chem. Soc. 116(1994) 2094-2102.

35. V. M. Geskin, C. Lambert and J. L. Bredas. J. Am. Chem. Soc. 125(2003) 15651-15658.

36. R. P. Singh, A. Sethi et al., J. Mol. Struct. 1105 (2016) 423-433.

37. D. A. Kleinman. Phys. Rev. 126 (1962) 1977.

38. J. S. Murray and K. Sen. Molecular Electrostatic Potentials, Concepts and Applications. Elsevier, Amsterdam; 1996.

39. J. P. Gallivan, D. A. Dougherty, Proc. Nat. Acad. Sci. USA, 96 (1999) 9459–9464.

40. K. C. Duggan, M. J. Walters, J. Musee, J. M. Harp, J. R. Kiefer, J. A. Oates, L. J. Marnett, J Bio. Chem., 285 (2010) 34950–34959.